AIAA JOURNAL
Vol. 36, No. 5, May 1998

Phenomenological Analysis of Shock-Wave Propagation in Weakly Ionized Plasmas

Igor V. Adamovich,* Vish V. Subramaniam,† and J. William Rich‡
Ohio State University, Columbus, Ohio 43210-1107
and
Sergey O. Macheret§
Princeton University, Princeton, New Jersey 08544

Shock propagation into weakly ionized gases shows several features differing markedly from conventional, nonionized-gas shock structure. Phenomenological analysis of general macroscopic features of the previously observed plasma shock effects allows only two possible interpretations: existence of an energy (momentum) flux toward the wave precursor or volumetric energy release (exothermic phase transition) in the upstream portion of the wave (precursor) followed by reverse transition in the downstream portion of the wave. It is shown that known microscopic mechanisms are not capable of producing such a flux or energy release: Typical processes involving electrons, ions, and excited species do not couple strongly to neutral atoms and molecules, and there is not enough energy stored in these species because of the low ionization fraction. The theoretical basis for phase transitions in low-density, weakly ionized plasmas also is unknown. Analysis of the steady two-wave system created by either of the two effects raises a question as to whether the observed plasma shocks are stable objects. Another question is whether there exists phase transition within the plasma shock. It also remains unclear to what extent two-dimensional thermal inhomogeneity effects contribute to the observed phenomena. Answering these fundamental questions requires additional experimental studies of the problem.

Nomenclature

c_p	= specific heat, J/kg/K
D	= diffusion coefficient, m^2/K
d	= shock separation, m
E	= electric field, V/m
E/N	= reduced electric field, V · m^2
e	= electron charge, C
F	= external force per unit area, N/m^2
h	= enthalpy, J/kg
j	= current density, A/m^2
k	= Boltzmann constant, J/K
k_{deexc}	= rate of atom deexcitation by electrons, cm^3/s
k_{exc}	= rate of atom excitation by electrons, cm^3/s
k_{ion}	= ionization rate, cm^3/s
k_{quench}	= rate of excited atom quenching by ground-state atoms, cm^3/s
k_{rec}	= recombination rate, cm^3/s
L	= spatial scale, m
l	= shock thickness, m
M	= shock Mach number
m	= species mass, kg
N	= concentration, m^{-3}
n	= species number density, m^{-3}
P	= pressure, Pa
Q	= heat addition, J/kg
$\tilde{Q}$	= $Q - q/\rho u$
q	= heat flux, W/m^2
S	= entropy, J/kg/K
T	= temperature, K
t	= time, s
u	= flow velocity, m/s
v_s	= shock velocity, m/s
W	= work by external force, J/kg
x	= axial coordinate, m
γ	= specific heat ratio
ε_a	= excited atom energy, K
ε_0	= dielectric permeability of vacuum, V · m/C
λ	= heat conductivity, W/m/K
μ	= dynamic viscosity, kg/m/s
ν	= collision frequency, s^{-1}
ξ	= Thompson heat coefficient, V/K
ρ	= density, kg/m^3
σ	= collision cross section, m^2
τ	= normal stress, N/m^2
φ	= electric potential, V
ω	= wave frequency, s^{-1}

Subscripts

A	= in front of a shock
a	= excited atom
B	= behind the shock
cr	= critical
e	= electron
en	= electron neutral
fin	= final
gd	= gasdynamic
i	= ion
in	= ion neutral
init	= initial
n	= neutral
tr	= transverse
1	= first (upstream) shock
2	= second (downstream) shock

Received April 16, 1997; revision received Jan. 2, 1998; accepted for publication Jan. 25, 1998. Copyright © 1998 by the American Institute of Aeronautics and Astronautics, Inc. All rights reserved.

*Research Scientist, Department of Mechanical Engineering, 206 West 18th Avenue. Senior Member AIAA.
†Associate Professor, Department of Mechanical Engineering, 206 West 18th Avenue. Senior Member AIAA.
‡Ralph W. Kurtz Professor, Department of Mechanical Engineering, 206 West 18th Avenue. Associate Fellow AIAA.
§Senior Research Scientist, D418 Engineering Quadrangle, Department of Mechanical and Aerospace Engineering. Senior Member AIAA.

I. Introduction

SHOCK-WAVE propagation in weakly ionized plasmas ($n_e/N \sim 10^{-8}$–10^{-6}) has been studied extensively for the past 15 years, mostly in Russia[1–11] and recently in the United States.[12] The following anomalous effects have been observed: 1) shock acceleration,

2) nonmonotonic variation of flow parameters behind the shock front, 3) shock weakening, and 4) shock-wave splitting and spreading. These effects, observed in discharges in various gases (air, CO_2, Ar, He) at pressures of 3–30 torr, and for Mach numbers $M \sim 1.5$–4.5, are surprisingly similar in both atomic and molecular gases, despite fundamental differences in mechanisms of ionization and molecular energy transfer. They also persist for a long time after the discharge is off (~1 ms in air[2,9]).

As is well known, shock-wave acceleration can be explained qualitatively by gas heating in the discharge and/or by energy relaxation of the species excited in a discharge. A number of models have been proposed that predict acceleration of the shock traveling in a vibrationally excited gas, e.g., moist nitrogen, or across an axial temperature gradient.[13–15] Energy relaxation models also predict nonmonotonic variation of flow parameters behind shocks in molecular gas plasmas. However, they fail to explain why these effects occur in monatomic gases such as argon, where much less energy is stored in the internal degrees of freedom. Further, the existing models do not explain effects 3 and 4, that is, anomalous shock absorption and dispersion. In the experiments at $P = 10$–30 Torr, the shock is observed to split into a series of two or more individual shocks at ionization fractions as low as $n_e/N \sim 10^{-8}$ (see Fig. 1, taken from Ref. 12). These individual shocks become separated by tens of millimeters at $n_e/N \sim 10^{-6}$ (see Fig. 2, taken from Ref. 9). We believe that understanding these effects, in particular, is the key to the whole problem. We analyze two stages of shock propagation in plasmas: initial shock-wave splitting and sustaining the steady-state system of two shocks. This very elementary analysis leads to some general conclusions as to the nature of the mechanism involved.

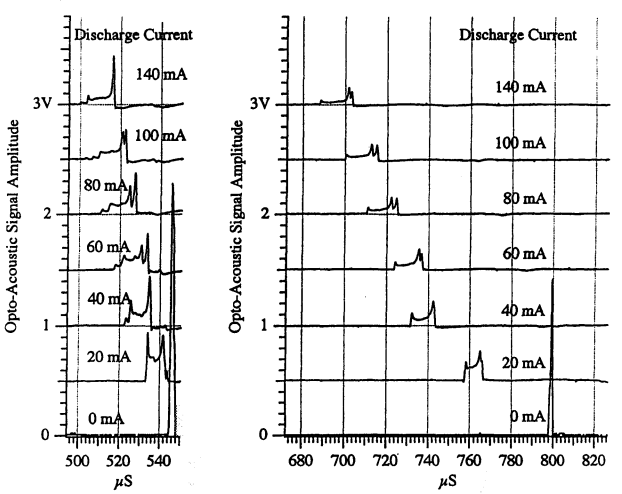

Fig. 1 Optoacoustic signal from a shock wave (density gradient) in a 30-torr axial glow discharge in argon[12] ($M \cong 1.7$). The discharge tube diameter is 5 cm.

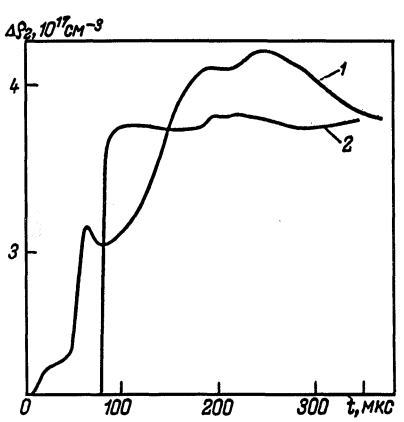

Fig. 2 Density profile across the plasma shock in transverse glow discharge in air ($T \cong 350$ K, $P = 12$ torr, initial shock velocity $v_s = 500$ m/s, $j_{tr} = 30$ mA/cm^2; 1, in plasma; 2, without plasma).

II. Shock-Wave Splitting

It is well known[16] that absorption and dispersion of a wave in a relaxing gas become important only when the product of the wave frequency and the relaxation time ωt is comparable to 1. For the initial regular shock, this can happen only if t is comparable to the gasdynamic collision time t_{gd}. Therefore, an energy relaxation process can affect the shock front structure (to produce wave dispersion) only if it occurs at frequencies equal to or greater than the gasdynamic collision frequency. Note that energy absorption would reduce the shock-wave speed, whereas only a release of energy would produce shock acceleration. Therefore, the energy must be released in the upstream part of the wave. It is also clear that whatever the mechanism is, a significant portion of the incident flow energy should be absorbed (or released) to considerably alter the shock strength and velocity. For these reasons, relaxation processes cannot be responsible for the shock absorption and dispersion. For most of these processes, e.g., vibrational and metastable species relaxation, chemical reactions, the characteristic time is far too long ($t \gg t_{gd}$) at the low gas temperatures involved. All electron and ion impact processes also happen on a much longer timescale because of the low ionization fraction. Finally, species that can be excited (or quenched) rapidly cannot store much energy. Slow relaxation processes might become important in the shock-wave energy balance only after the wave front transforms from a well-defined shock to a dispersive structure, so that lower harmonics appear in the wave Fourier integral. For example, for $v_s = 1$ km/s and $t \sim 10^{-4}$ s (characteristic time for collisional vibration–vibration exchange in air at $P = 10$ torr, $T = 300$ K), the absorption and dispersion would be maximum for a shock thickness of $l \sim 10$ cm (at least 10^3 mean free paths). Similarly, the characteristic ionization/recombination scale is $l \sim v_s/k_{rec}n_e \sim l - 100$ cm.

Energy addition by a discharge as well as discharge-related instabilities (heating instability, stepwise ionization instability, etc.) can be ruled out as possible mechanisms of shock splitting for two reasons. One is that, again, all of these processes in weakly ionized plasmas are far too slow compared to the heating rate in a shock wave.[17] The other is that the observed plasma shock effects persist after the discharge is off. For a glow discharge in air at $P = 10$ torr, $T = 300$ K, $j = 100$ mA/cm^2, $E = 100$ V/cm ($n_e/N \sim 10^{-6}$, $E/N \sim 3 \times 10^{-16}$ V·cm^2, $T_e \sim 1$ eV) one has $dT/dt \sim 10^6$ K/s (gas heating in an $M = 2$ shock occurs at a rate of $\sim 10^9$ K/s). The characteristic spatial scale for the discharge energy addition is $l \sim 10$ cm.

Finally, experiments involving strong shocks ($M \sim 4$) (Ref. 10) have shown that the shock-splitting mechanism is definitely self-feeding and cannot be due to the discharge energy addition. Well-pronounced shock spreading, to over ~100 mm, and acceleration have been observed in cold air plasmas even when the energy addition by a discharge was about 25 times less than the shock stagnation enthalpy (~50 J/g vs ~1300 J/g). At these conditions, the only energy reservoir available was the incident flow kinetic energy.

We conclude that the observed simultaneous shock dispersion and acceleration might be sustained by a kinetic process that absorbs energy behind the shock, transports it across the shock front, and adds energy ahead of the shock front. This suggestion is consistent with observations of fast-moving precursors ahead of the shock front. This process must meet the following requirements:

1) The velocity of the energy carriers should be greater than the shock velocity.

2) The energy should be absorbed and released sufficiently fast ($t \leq t_{gd}$).

3) The energy reservoir must not be related to the discharge.

4) The resultant energy flux should be comparable to that of the shock wave.

By this process, the precursor ahead of the shock can be sustained by the remainder of the shock wave.

III. Steady-State Two-Wave Systems

For analysis of steady-state finite amplitude perturbations in plasmas (plasma shocks), we use the one-dimensional conservation equations of mass, momentum, and energy of a fluid in a reference frame moving with the wave[18]:

$$\Delta(\rho u) = 0$$

$$\Delta(\rho u^2 + P) = (\tau_{\text{fin}} - \tau_{\text{init}}) + F \tag{1}$$

$$\Delta(u^2/2 + h) = [(\tau_{\text{fin}} u_{\text{fin}} - \tau_{\text{init}} u_{\text{init}}) - (q_{\text{fin}} - q_{\text{init}})]/\rho u + W + Q$$

In Eqs. (1), the normal stress τ and the heat flux q exist in the flow due to as-yet unspecified effects. The subscripts init and fin refer to conditions in front of and behind the wave. Note that this system is written for the whole flow, rather than for each species present in the flow. It therefore does not matter whether the flow is ionized or not, as long as the presence of the charged component does not significantly change both the thermal ($P = \rho kT/m$) and the caloric ($h = c_p T$) equations of state, which is true for weakly ionized plasmas. For steady adiabatic conditions, $\tau_{\text{fin}} = \tau_{\text{init}} = q_{\text{fin}} = q_{\text{init}} = T = W = Q = 0$, one always obtains the Rankine–Hugoniot relations across the steady perturbation, regardless of the nature of τ and q or what happens within the perturbation region.

In classical gasdynamics, two normal (adiabatic) shocks cannot travel at the same velocity because the flow behind the upstream shock is always subsonic. However, such shocks can exist if they are allowed to exchange energy with each other while remaining globally adiabatic. Let us consider such a globally adiabatic system of two locally nonadiabatic normal shocks. Let us also assume for simplicity that the waves cannot exchange momentum and that there are no external forces. In Fig. 3, we consider a control volume around each wave, and an outer control volume comprising the far field, where all flow parameters are constant. For each wave, the system of Eqs. (1) is applicable:

$$\rho_{1B} u_{1B} = \rho_{1A} u_{1A} = \rho_{2B} u_{2B} = \rho_{2A} u_{2A}$$

$$\rho_{1B} u_{1B}^2 + P_{1B} = \rho_{1A} u_{1A}^2 + P_{1A} = \rho_{2B} u_{2B}^2 + P_{2B} = \rho_{2A} u_{2A}^2 + P_{2A}$$

$$Q_1 = -Q_2 = Q \tag{2}$$

$$q_{1B} = q_{2A} = q$$

$$\begin{cases} u_{1B}^2/2 + c_p T_{1B} - u_{1A}^2/2 - c_p T_{1A} = Q - q/\rho u = \tilde{Q} \\ u_{2B}^2/2 + c_p T_{2B} - u_{2A}^2/2 - c_p T_{2A} = -Q + q/\rho u = -\tilde{Q} \end{cases}$$

Solutions of Eqs. (2), which determine the Rayleigh line on the T-S diagram (Fig. 4), are well known. They demonstrate the following features:

1) Both perturbations are compression waves only when $\tilde{Q} > 0$ (wave 1 absorbs energy, $S_{1B} > S_{1A}$). Note that this is the typical situation observed in experiments on plasma shocks; the existence of an entropy overshoot can be inferred from the simultaneously measured density and pressure profiles in a plasma shock.[9,10] If $\tilde{Q} < 0$, one of the perturbations is always a rarefaction wave. From now on, we assume that $\tilde{Q} > 0$.

2) If $\tilde{Q} < \tilde{Q}_{\text{cr}}$, where

$$\tilde{Q}_{\text{cr}} = c_p T_{1A} \frac{(M_{1A}^2 - 1)^2}{2(\gamma + 1) M_{1A}^2} \tag{3}$$

there exist two different solutions for the flow parameters between the waves (Fig. 4); sonic transition can occur in either wave 1 or wave 2. If $\tilde{Q} = \tilde{Q}_{\text{cr}}$, the solution is unique and the flow between the waves is sonic. For $\tilde{Q} > \tilde{Q}_{\text{cr}}$, there is no steady solution.

It is evident that $\tilde{Q}$ should be comparable to the incident flow enthalpy $c_p T_{1A}$ in order to change substantially the shock strength

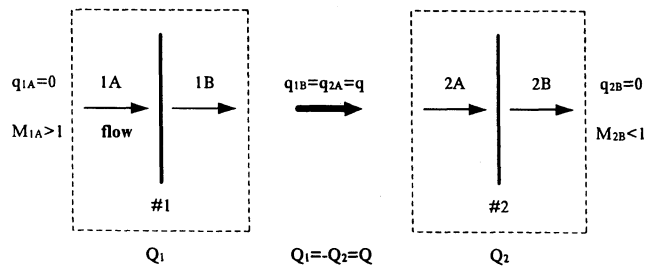

Fig. 3 Steady globally adiabatic system of two waves.

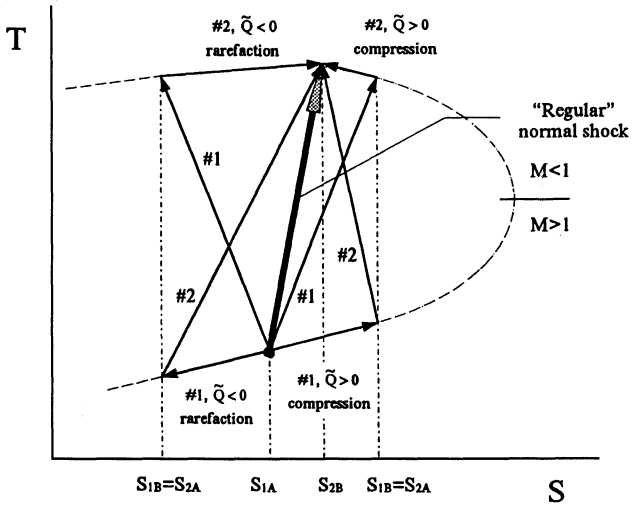

Fig. 4 T-S diagram of steady two-wave system.

ρ_B/ρ_A. To reduce the shock strength at $M = 2$ in argon at $T = 300$ K and $P = 10$ torr by half, the magnitude of the heat source/sink should be $Q \sim \tilde{Q} \sim 0.35 \cdot c_p T_{1A} = 55$ J/g, or, alternatively, the magnitude of the heat flux should be $q \sim \tilde{Q}\rho u \sim 75$ W/cm^2. At $M = 4$, $Q \sim 1.9 \cdot c_p T_{1A} = 280$ J/g and $q \sim 760$ W/cm^2.

The two-shock system also can be analyzed using the one-dimensional Navier–Stokes equations, including both regular transport phenomena (viscosity and heat conduction) and anomalous heat flux/source. These equations are the one-dimensional differential forms of Eqs. (2). Because the nature of Q and q in these equations is unknown, they are treated phenomenologically, by imposing a spatial distribution for these quantities.

In these calculations, the width of the heat addition/loss regions was varied, the quantity $\tilde{Q} = Q_1 = -Q_2 = 0.3 \cdot c_p T_{1A}$ was kept constant, and global adiabaticity of the flow was preserved ($Q_1 + Q_2 = 0$). One of the two steady solutions is obtained, depending on the initial conditions (Fig. 5). It can be seen that, for $\tilde{Q} < \tilde{Q}_{\text{cr}}$, the steady system of two compression waves always consists of a discontinuous shock with a thickness on the order of the mean free path and a compression wave the thickness of which is determined by the width of local heat addition/loss region (Figs. 5a and 5b). This is exactly what has been observed in experiments[9,10] (Fig. 2). Note that a compression wave (subsonic-to-subsonic or supersonic-to-supersonic), where heat is added to or removed from the flow sufficiently fast (on a timescale comparable to the heating in a regular shock) may look like a shock (see Fig. 5a). At $\tilde{Q} = \tilde{Q}_{\text{cr}}$ the flow discontinuity disappears, and a shockless transition to a subsonic flow is realized (classical Rayleigh flow).

When a regular shock wave decomposes into a system of two energy-exchanging waves in a globally adiabatic flow, the density behind this unsteady shock is greater than its steady-state value (Fig. 6). Comparing Figs. 2 and 6, one can see that, under the conditions of the experiments of Ref. 9, this effect should occur about $t = 0.35 \cdot L/v_s = 1.75 \cdot d/v_s \sim 200$ μs after the shock encounters the plasma. Here $d \sim 50$ mm is the shock separation (Fig. 2), and $L = 5d$ is the spatial scale (see Fig. 6). Indeed, the interferometric measurements in Ref. 9 were made at a distance of 150 mm from the discharge boundary, so that the shock residence time in the plasma was $\sim$300 μs. This shows that the observed density and pressure increase behind plasma shocks in air[9,10] are due to unsteadiness of the flow at the initial stage of the shock splitting. The same effects occur in steady but globally nonadiabatic flows, where density and static pressure behind the cooled ($Q_1 + Q_2 < 0$) two-wave system increase compared to the values given by the Rankine–Hugoniot relations.

Note that all of these results are independent of the mechanism of heat addition/loss and heat transfer. If the two waves exchange momentum and external forces are present, the qualitative features of the solutions of the governing equations, which then would define the Fanno lines on the T-S diagram, would be the same as described earlier.

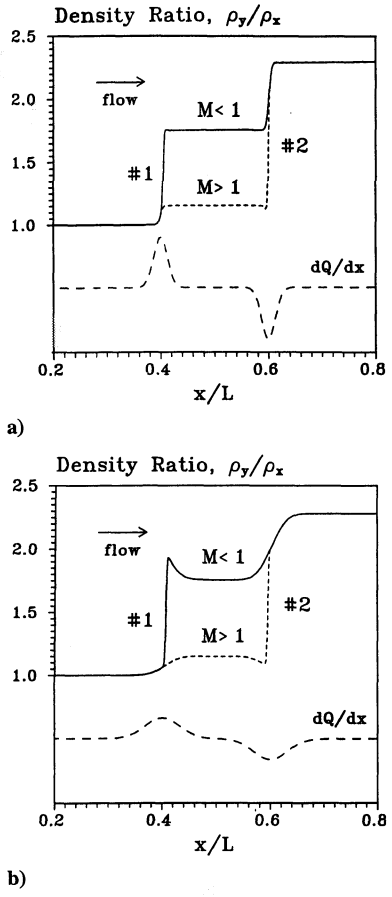

Fig. 5 Steady-state density profiles in a globally adiabatic system of two interacting shocks (argon at T_{1A} = 300 K, P_{1A} = 10 torr, M_{1A} = 2, L = 10 mm, $Q = 0.3 \cdot c_p T_{1A}$): a) narrow and b) wide energy release/absorption zones (shown at bottom).

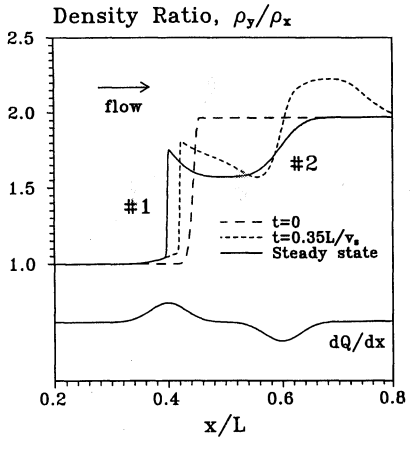

Fig. 6 Time-dependent density profiles for a two-shock system shown in Fig. 5b.

This analysis suggests that there are only two possible explanations for the steady plasma shock:

1) anomalous heat and/or momentum flux from the downstream wave to the upstream wave ($q = 10^2$–10^3 W/cm^2 at $P \sim 10$ torr), in which case, however, it is unclear what controls the wave separation;

2) volumetric heat addition (exothermic phase transition) in the upstream wave followed by the reverse endothermic process in the downstream wave ($Q \sim 10^2 - 10^3$ J/g at $P \sim 10$ torr), a mechanism known to produce shock-wave splitting in solids.[19] In this case no anomalous fluxes are present, but the caloric and the thermal equation of state change, and the wave separation is determined by the lifetime of the new phase.

IV. Possible Microscopic Mechanisms

Given the results of Sections II and III, let us consider some scenarios to see if they are feasible. Let us first discuss energy transfer by charged species, ion-acoustic wave and electron heat conduction.

A. Energy Transfer Due to Motion of Charged Species

To study these processes, we developed a one-dimensional hydrodynamic kinetic model of shock-wave propagation in weakly ionized nonequilibrium plasma. It incorporates Navier–Stokes equations for a viscous, heat-conducting gas consisting of the ground state and excited neutral species, and Navier–Stokes-type equations for charged species obtained from the Boltzmann equation in the hydrodynamic approximation[20] (see Appendix). The plasma is not assumed to be quasineutral, and the Poisson equation for the electric field also is incorporated. The coupling between the charge carriers and the heavy species is described by heating and drag in electron-neutral and ion-neutral collisions.

Because the observed plasma shock effects are very similar in both atomic and molecular gases (see Section I), we limit the analysis to argon plasma. The simplified kinetic model incorporates the following energy transfer processes:

$$\mathrm{Ar} + e \leftrightarrow \mathrm{Ar} + e \text{ (elastic)} \tag{4}$$

$$\mathrm{Ar} + e \leftrightarrow \mathrm{Ar}^+ + e + e \tag{5}$$

$$\mathrm{Ar} + e \leftrightarrow \mathrm{Ar}^* + e \tag{6}$$

$$\mathrm{Ar}^* + \mathrm{Ar} \rightarrow \mathrm{Ar} + \mathrm{Ar} \tag{7}$$

In Eq. (6), Ar* is an excited metastable atom Ar(^{3}P) with the energy of about 12 eV. The electron-neutral elastic collision frequency ν_{en}, the rates of ionization k_{ion}, recombination k_{rec}, and atom excitation and deexcitation by electrons k_{exc} and k_{deexc} were calculated separately by solving the Boltzmann equation[21] for electron energy distribution function in Ar, and incorporated into the model as functions of electron temperature. The rate of excited-atom quenching by the ground-state atoms, k_{quench}, was taken from Ref. 22. The effects of vibrational excitation and relaxation, important in molecular plasmas, can be included easily on the basis of our other existing kinetic models for N_2 and air,[23,24] which already incorporate the Boltzmann equation for electrons.

Some of the steady-state results obtained for the transverse discharge in Ar with the model described above are presented in Figs. 7–9. The flow and the discharge parameters are $P = 10$ torr, $T = 300$ K, $M = 2$ ($v_s = 645$ m/s), $j_{tr} = 100$ mA/cm^2, $E_{tr}/N = 2 \times 10^{-16}$ V · cm^2, $n_e/N \cong 10^{-6}$, $n_a/N \cong 10^{-3}$, $T_e \cong 3.6$ eV.

In Figs. 7 and 8, one can see a structure ahead of the shock front, or the ion-acoustic wave. The electron and ion concentration distributions within this structure are in very good agreement with an analytic result,[25] obtained for the quasineutral plasma. This wave can

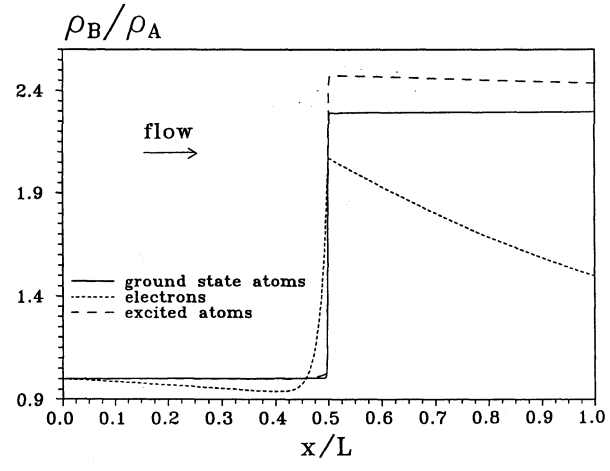

Fig. 7 Calculated steady-state species density distributions across the shock for transverse electric discharge in argon plasma. (P = 10 torr, T = 300 K, M = 2, j_{tr} = 100 mA/cm^2, E_{tr} = 60 V/cm, $T_e \sim 3.6$ eV, $n_e/N \sim 10^{-6}$, $n_a/N \sim 10^{-3}$, L = 10 mm.) Note the electron density dip ahead of the ion-acoustic wave.

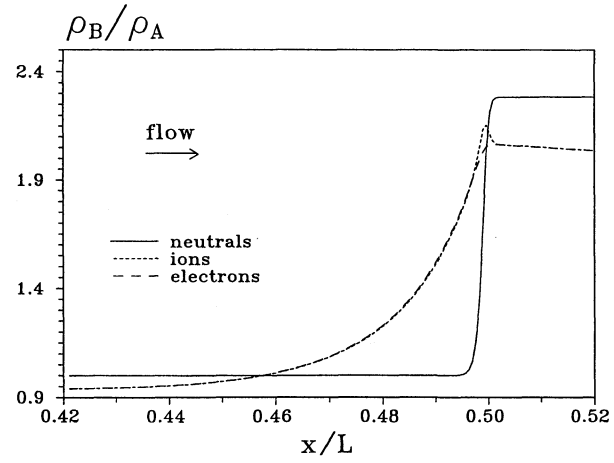

Fig. 8 Blown-up central section of Fig. 7.

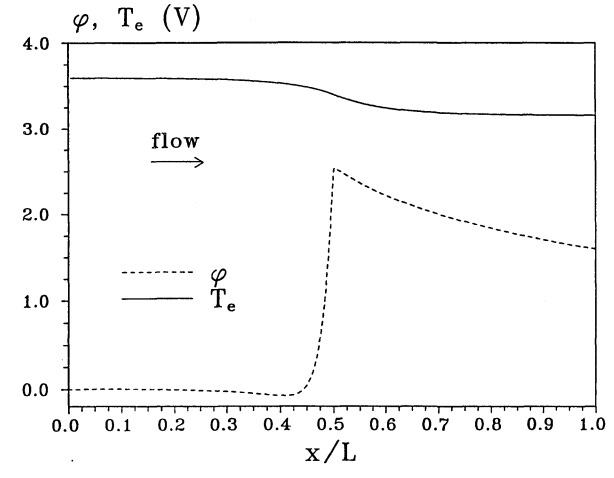

Fig. 9 Calculated steady-state electron temperature and potential distributions across the shock for the conditions of Fig. 7.

propagate forward at an ion sound velocity $\sim(kT_e/m_i)^{1/2} \sim 2700$ m/s.[25] In particular, the electrons are pushed forward by the electron pressure gradient in the shock, and decelerated by the induced electric field. Note that this electric field tends to stop the electrons, i.e., reduces their kinetic energy, and so, it cannot produce field-related ionization. It is the ions that are accelerated by this field. The ions are being stopped by the ion-neutral drag, which is the principal mechanism of the ion-acoustic wave damping. The potential drop across the shock, $\Delta\varphi \sim T_e$ (Fig. 9), is equal to the energy acquired by the ions and eventually lost in the ion-neutral collisions. In all of our calculations, the potential drop did not exceed $\Delta\varphi \sim 5$ eV. This result is in qualitative agreement with the potential drop measurements across plasma shocks in air,[3] showing, as expected, that the electron temperatures in both cases are comparable. One can estimate that the maximum energy flux transmitted by the ion-acoustic wave is $q \sim n_i(kT_e/m_i)^{1/2}kT_i \sim 10^{-3}$ W/cm^2, which is about five orders of magnitude less than required (see Sec. III). Therefore, the ion-acoustic wave, although much faster than the shock wave, cannot transport enough energy to decompose the shock.

From Fig. 9, one can also see that the electron temperature behind the shock drops by about 10%. This occurs because the gas density there is greater and the reduced electric field E_{tr}/N is less, so that the electron heating by the field, as well as ionization, becomes slower. In fact, a complete discharge extinguishing is observed a few centimeters behind the shock wave. This effect is somewhat reduced by the energy transfer from the excited Ar atoms back to electrons in superelastic collisions [Eq. (6)]. The decrease in electron temperature behind the shock has been observed in the calculations in a range of Mach numbers $M = 1.5$–5, $E_{tr}/N = 1 \times 10^{-16}$–$5 \times 10^{-16}$ V · cm^2, and $n_e/N = 10^{-8}$–10^{-6}. It is also expected that a similar result will be obtained in N_2 and air. Indeed, solution of the Boltzmann equation[26,27] shows that the electron temperature and the ionization rate in nitrogen always increase with E/N in the reduced electric field range that is considered, even though the energy transfer from vibrationally excited molecules to electrons tends to increase T_e and k_{ion} at the low values of $E/N \sim 10^{-16}$ V · cm^2 and high vibrational temperatures $T_v \sim 0.2$–0.4 eV.[27] Because of the large electron heat conductivity, the electron temperature and, consequently, the ionization rate and the electron concentration ahead of the shock also decrease (Fig. 9). In particular, this means that the electron heat conduction cannot trigger the ionization instability in the precursor. Note that this result is also consistent with experimental measurements of plasma conductivity and electron concentration ahead of plasma shocks in air,[3,5] which show the dip in values of both of these parameters ahead of the shock.

The maximum heat flux that can be transmitted by the electrons is $q_e \sim n_e(kT_e/m_e)^{1/2}kT_e$. For the discharge parameters considered, $n_e \sim 3 \times 10^{11}$ cm^{-3} and $T_e \sim 3.6$ eV, one has $q_e \sim 10$ W/cm^2. As expected, electron heat conduction might be capable of producing the required heat flux. Because the energy stored in the electrons is minute, the electron heat flux must be strongly coupled with some energy reservoir, e.g., external electric field or excited species. We already saw that this coupling, which limits the amount of energy transferred by electrons, actually results in an electron heat flux downstream, i.e., in the opposite direction (Fig. 9). The magnitude of this heat flux is $q_e = (n_e/N)\lambda_e\,(dT_e/dx) \sim 10^{-1}$ W, which is about three orders of magnitude lower than required. The small value of the electron heat flux is due primarily to the existence of the quasisteady state between rapid excitation and deexcitation of Ar atoms by electrons in process (6), the net energy flow toward electrons being fairly slow. The same qualitative result is expected in N_2 and air, where the cross sections of both electron-impact vibrational excitation and superelastic deexcitation are quite large ($\sigma \sim 10^{-16}$ cm^2),[27] which would result in a similar quasisteady state.

Thus, the coupling of electron heat conduction with the electric field and species excited in a discharge also fails to provide the necessary heat flux. Also note that this type of coupling requires energy addition by a discharge, and therefore cannot explain the dispersion of strong shocks (see discussion in Sec. II). Without an extremely fast coupling between electrons and the neutral species, any heat transfer mechanism involving motion of charged species, e.g., ion-acoustic waves, plasma instabilities, oscillations and waves, plasma turbulence, becomes irrelevant to the plasma-shock problem. Even though some of these processes do result in charged species precursor formation in front of the shock, their effect on the neutral species remains extremely weak.

B. Energy Transfer by Hot Atoms and Molecules

Translationally hot heavy species appear in nonequilibrium plasmas as products of relaxation processes, such as given by Eq. (7), where they may acquire large kinetic energies. These could travel rapidly across the thin shock layer and translationally relax, i.e., heat the gas, in front of it. However, thermalization normally requires just a few collisions, and so, the observed large separation between the shocks cannot be explained.

C. Electromagnetic Radiation

The gas flow in the plasma shock is relatively cold ($T < 1500$–2000 K). The blackbody radiation flux, being far from negligible ($q \sim T^4 \sim 1$ W/cm^2 at $M = 2$, $q \sim 75$ W/cm^2 at $M = 4$), is still not large enough. Besides, a weakly ionized cold plasma is transparent. The electromagnetic-wave absorption coefficient at these conditions is extremely small. One can speculate on the possibility of microwave radiation and absorption by the neutral species because of their translational motion, with the dipole moment induced by the charge separation in the shock front. The wavelength of this continuous radiation, similar to that which occurs in high-pressure gases and liquids, is ~15–50 μm. However, the estimated induced dipole moment, as well as the number density of induced dipoles, is vanishingly small to explain the observed effects.

Radiation from excited species also can be ruled out. Radiating electronic states are populated in a discharge by electron impact, and the resultant energy flux can reach ~1 W/cm^2. However, this mechanism, based on the discharge-energy addition, again does not provide coupling with the bulk of the flow energy and cannot explain the spreading of strong shocks (see Sec. II).

D. Thermoelectric Effects

The presence of weak levels of ionization in the plasma-shock problem is somewhat reminiscent of the behavior of charge carriers across semiconductor p-n junctions.[28] Thermoelectric phenomena such as Peltier heat and Thompson heat could be relevant. The Thompson heat per unit mass, $dQ/dx = \xi(j \times \text{grad } T)/\rho u$, is due to a reversible volumetric heating/cooling mechanism. Because the Thompson heat scales linearly with the current density whereas the Ohmic heating is proportional to j^2, it is relevant only for low current densities. However, the Thompson heat can be comparable to the required heat addition estimated above only if $\xi \sim 10$ V/K (for $j = 100$ mA/cm^2). This is several orders of magnitude greater than the values of μ_T measured in semiconductors.[28] Also, the Thompson effect requires the presence of the discharge current and cannot explain the shock dispersion after the discharge is off.

E. Non-One-Dimensional Effects

At this moment, we cannot rule out the possibility that the observed plasma shock effects are simply due to the distortion of a plane shock-wave front propagating in a region with a transverse temperature gradient. Indeed, two-dimensional inviscid calculations[29] demonstrate this kind of distortion and the shock spreading within a heated cathode layer of a transverse pulsed discharge in air.[10] The gas temperature distribution in the experiment[10] has been measured by optical interferometry. Similar calculations performed at Princeton University using two-dimensional inviscid code[30] also showed shock dispersion by the transverse temperature gradient.[31] However, neither of these calculations shows any shock splitting outside the heated layer, in a cold plasma flow, where it has been measured experimentally.[10]

It remains unclear how much the spatially inhomogeneous gas heating by a discharge contributed to the shock-wave distortion in the experiments.[1-12] This can be clarified by additional transverse temperature distribution measurements and two-dimensional Navier–Stokes modeling of shock-wave propagation in a nonhomogeneous plasma region.

F. Phase Transitions

At present, we are not aware of any theoretical bases for phase transitions in low-density weakly ionized nonequilibrium plasmas. Because the relaxation of energy stored in the internal degrees of freedom already has been ruled out, the only remaining possibility here is changing the intermolecular interaction, i.e., condensation. The idea of formation of a polymer structure with anomalous properties, e.g., surface tension, elasticity, high speed of sound, in the plasma shock has been discussed in the Russian literature.[32] Some data (anomalous absorption of 10.4-μm and 0.3-mm laser radiation in the plasma shock[32]) appear to support this hypothesis. However, these experiments have not been reproduced elsewhere. The phenomenological approach used in the present paper does not allow any further analysis of this phase-transition hypothesis, which at this moment remains pure speculation.

V. Summary and Conclusions

Analysis of general macroscopic features of the observed plasma shock effects (shock dispersion) allows only two possible phenomenological interpretations:

1) Heat and/or momentum flux, comparable to the incident-flow energy flux, from the downstream wave toward the upstream wave (precursor).

2) Volumetric heat addition (exothermic phase transition) in the precursor with a latent heat comparable to the incident-flow enthalpy, followed by a reverse endothermic process in the downstream wave.

None of the known microscopic mechanisms is capable of producing such a flux. Typical processes involving electrons, ions, and excited species do not couple strongly to neutral atoms and molecules; moreover, there is not enough energy stored in these species because of the low ionization fraction. There is also no known theoretical basis for phase transitions in low-density nonequilibrium plasmas.

Existence of double-valued solutions for the steady two-wave structures for $\tilde{Q} < \tilde{Q}_{cr}$, as well as absence of the steady solution for $\tilde{Q} > \tilde{Q}_{cr}$, created by either of the two aforementioned effects, raises the question as to whether the observed plasma shocks are indeed stable objects. Another question is whether there exists any condensation or cluster formation within the plasma shock. Finally, the suggested method does not allow analysis of the effect of two-dimensional flow inhomogeneity on the shock-wave structure. Recent calculations show that a strong transverse temperature gradient might cause shock-front distortion and splitting. It is not clear, however, to what extent this purely thermal effect contributed to the observed phenomena.

Answering these fundamental questions might clarify the nature of the plasma shock phenomena. This will require measuring the gas density distribution and the infrared emission (absorption) spectrum across the shock, in a controlled environment where the shock is stationary and with good spatial and time resolution.

Appendix: One-Dimensional Monatomic Plasma Flow Equations

Ground-State Atoms

$$\frac{\partial n}{\partial t} + \frac{\partial (Nu)}{\partial x} = 0$$

$$\frac{\partial u}{\partial t} + u\frac{\partial u}{\partial x} = -\frac{1}{m_n N}\frac{\partial P}{\partial x} + \frac{1}{m_n N}\frac{\partial}{\partial x}\left(\frac{4}{3}\mu_n \frac{\partial u}{\partial x}\right) + \nu_{en}(u_e - u)\frac{2m_e}{m_n}\frac{n_e}{N} + \nu_{in}(u_i - u)\frac{n_i}{N}$$

$$\frac{3}{2}\left(\frac{\partial T}{\partial t} + u\frac{\partial T}{\partial x}\right) = -T\frac{\partial U}{\partial x} + \frac{1}{Nk}\frac{\partial}{\partial x}\left(\lambda_n \frac{\partial T}{\partial x}\right) + \frac{4}{3}\frac{\mu_n}{Nk}\left(\frac{\partial u}{\partial x}\right)^2 + \frac{3}{2}\nu_{en}T_e\frac{2m_e}{m_n}\frac{n_i}{N} + \frac{3}{2}\nu_{in}(T_i - T)\frac{n_i}{N} + \varepsilon_a \cdot k_{quench} n_a N$$

$$P = NkT$$

Excited Atoms

$$\frac{\partial n_a}{\partial t} + \frac{\partial (n_a u_a)}{\partial x} = \frac{\partial}{\partial x}\left(D_n \frac{\partial n_a}{\partial x}\right) + k_{exc} N n_e - k_{deexc} n_a n_e - k_{quench} n_a N$$

Ions

$$\frac{\partial n_i}{\partial t} + \frac{\partial (n_i u_i)}{\partial x} = k_{ion} N n_e - k_{rec} n_e n_i$$

$$\frac{\partial u_i}{\partial t} + u_i\frac{\partial u_i}{\partial x} = -\frac{1}{m_i n_i}\frac{\partial P_i}{\partial x} + \frac{1}{m_i n_i}\frac{\partial}{\partial x}\left(\frac{4}{3}\mu_i \frac{\partial u_i}{\partial x}\right) + \frac{e}{m_i}E - \nu_{in}(u_i - u)$$

$$\frac{3}{2}\left(\frac{\partial T_i}{\partial t} + u_i\frac{\partial T_i}{\partial x}\right) = -T_i\frac{\partial u_i}{\partial x} + \frac{1}{n_i k}\frac{\partial}{\partial x}\left(\lambda_i \frac{\partial T_i}{\partial x}\right) + \frac{4}{3}\frac{\mu_i}{n_i k}\left(\frac{\partial u_i}{\partial x}\right)^2 - \frac{3}{2}\nu_{in}(T_i - T)$$

$$P_i = n_i k T_i$$

Electrons

$$\frac{\partial n_e}{\partial t} + \frac{\partial (n_e u_e)}{\partial x} = k_{ion} N n_e - k_{rec} n_e n_i$$

$$\frac{\partial u_e}{\partial t} + u_e\frac{\partial u_e}{\partial x} = -\frac{1}{m_e n_e}\frac{\partial P_e}{\partial x} + \frac{1}{m_e n_e}\frac{\partial}{\partial x}\left(\frac{4}{3}\mu_e \frac{\partial u_e}{\partial x}\right) - \frac{e}{m_e}E - \nu_{en}(u_e - u)$$

$$\frac{3}{2}\left(\frac{\partial T_e}{\partial t} + u_e\frac{\partial T_e}{\partial x}\right) = -T_e\frac{\partial u_e}{\partial x} + \frac{1}{n_e k}\frac{\partial}{\partial x}\left(\lambda_e \frac{\partial T_e}{\partial x}\right) + \frac{4}{3}\frac{\mu_e}{n_e k}\left(\frac{\partial u_e}{\partial x}\right)^2 + \left[\frac{e^2 E_{TR}^2}{m_e k \nu_{en}^2} - \frac{3}{2}\left(\frac{2m_e}{m_n}\right)T_e\right]\nu_{en} - \varepsilon_a(k_{exc} N n_e - k_{deexc} n_a n_e)$$

$$P_e = n_e k T_e$$

Poisson Equation

$$\frac{dE}{dx} = \frac{e}{\varepsilon_0}(n_i - n_e)$$

Transport Coefficients and Kinetic Rates

$$ND_n = 5.42 \times 10^{20}(T/300)^{0.75}\ \mathrm{m^{-1}/s}$$

$$\mu_i \cong \mu_n = 2.22 \times 10^{-5}(T/300)^{0.75}\ \mathrm{kg \cdot s/m}$$

$$\lambda_i \cong \lambda_n = 1.78 \times 10^{-2}(T/300)^{0.75}\ \mathrm{W/m/K}$$

$$ND_e = 7.3 \times 10^{24}\ \mathrm{1/m/s}$$

$$\mu_e = 4.3 \times 10^{-6}\ \mathrm{kg \cdot s/m}$$

$$\lambda_e = 2.4 \times 10^{2}\ \mathrm{W/m \cdot K}$$

$$\sigma_{\mathrm{in}} \cong \sigma_{\mathrm{nn}} = 6.0 \times 10^{-15}\ \mathrm{cm^2}$$

$$\nu_{\mathrm{in}} = N\left(\frac{8kT_i}{\pi m_i}\right)^{\frac{1}{2}}\sigma_{\mathrm{in}}$$

$$\nu_{\mathrm{en}} = \left[4.09 + 0.14(E_{\mathrm{tr}}/N) + 5.21 \times 10^{-3}(E_{\mathrm{tr}}/N)^2\right] \times 10^{12}$$

$$= \left(18.07 - 8.44T_e + 1.28 \times T_e^2\right) \times 10^{12}\ \mathrm{s^{-1}}$$

$$k_{\mathrm{ion}} = \exp[-22.69 - 15.80/(E_{\mathrm{tr}}/N)]$$

$$= \exp\left(-417.8 + 3240/T_e - 6684/T_e^2\right)\mathrm{cm^3/s}$$

$$k_{\mathrm{rec}} = 3.5 \times 10^{-8}\ \mathrm{cm^3/s}$$

$$k_{\mathrm{exc}} = \exp[-22.18 - 3.18/(E_{\mathrm{tr}}/N)]$$

$$= \exp\left(-32.99 + 145.9/T_e - 418.8/T_e^2\right)\mathrm{cm^3/s}$$

$$k_{\mathrm{deexc}} = 2.3 \times 10^{-8}\ \mathrm{cm^3/s}$$

$$k_{\mathrm{quench}} = 1.0 \times 10^{-15}\ \mathrm{cm^3/s}$$

$$\left[E_{\mathrm{tr}}/N = (0.5 - 6.0) \times 10^{-16}\ \mathrm{V \cdot cm^2}, \qquad T_e = 3.0\text{–}4.2\ \mathrm{eV}\right]$$

Acknowledgments

This work was sponsored by NASA as part of the MARIAH program. We would like to express our gratitude to B. N. Ganguli and P. Bletzinger for making available the results of their plasma shock experiments, and we thank D. M. Bushnell for numerous fruitful discussions.

References

[1]Klimov, A. I., Koblov, A. N., Mishin, G. I., Serov, Y. L., and Yavor, I. P., "Shock Wave Propagation in a Glow Discharge," *Soviet Technical Physics Letters*, Vol. 8, No. 4, 1982, pp. 192–194.

[2]Klimov, A. I., Koblov, A. N., Mishin, G. I., Serov, Y. L., Khodataev, K. V., and Yavor, I. P., "Shock Wave Propagation in a Decaying Plasma," *Soviet Technical Physics Letters*, Vol. 8, No. 5, 1982, pp. 240, 241.

[3]Basargin, I. V., and Mishin, G. I., "Probe Studies of Shock Waves in the Plasma of a Transverse Glow Discharge," *Soviet Physics—Technical Physics Letters*, Vol. 11, No. 11, 1985, pp. 535–538.

[4]Gorshkov, V. A., Klimov, A. I., Mishin, G. I., Fedotov, A. B., and Yavor, I. P., "Behavior of Electron Density in a Weakly Ionized Nonequilibrium Plasma with a Propagating Shock Wave," *Soviet Physics—Technical Physics*, Vol. 32, No. 10, 1987, pp. 1138–1141.

[5]Ershov, A. P., Klishin, S. V., Kuzovnikov, A. A., Ponomareva, S. E., and Pyt'ev, Y. P., "Application of the Reduction Method to the Microwave Interferometry of Shock Waves in Weakly Ionized Plasma," *Soviet Physics—Technical Physics*, Vol. 34, No. 8, 1989, pp. 936, 937.

[6]Basargin, I. V., and Mishin, G. I., "Precursor of Shock Wave in Glow-Discharge Plasma," *Soviet Technical Physics Letters*, Vol. 15, No. 4, 1989, pp. 311–313.

[7]Bystrov, S. A., Zaslonko, I. S., Mukoseev, Y. K., and Shugaev, F. V., "Precursor Ahead of a Shock Front in an RF Discharge Plasma," *Soviet Physics—Doklady*, Vol. 35, No. 1, 1990, pp. 39, 40.

[8]Mishin, G. I., Serov, Y. L., and Yavor, I. P., "Flow Around a Sphere Moving Supersonically in a Gas-Discharge Plasma," *Soviet Technical Physics Letters*, Vol. 17, No. 6, 1991, pp. 413–416.

[9]Mishin, G. I., Klimov, A. I., and Gridin, A. Y., "Measurements of the Pressure and Density in Shock Waves in a Gas Discharge Plasma," *Soviet Technical Physics Letters*, Vol. 17, No. 8, 1992, pp. 602–604.

[10]Gridin, A. Y., Klimov, A. I., and Khodataev, K. V., "Propagation of Shock Waves in a Nonuniform Transverse Pulsed Discharge," *High Temperature (USSR)*, Vol. 32, No. 4, 1994, pp. 454–457.

[11]Bedin, A. P., and Mishin, G. I., "Ballistic Studies of the Aerodynamic Drag on a Sphere in Ionized Air," *Soviet Technical Physics Letters*, Vol. 21, No. 1, 1995, pp. 5–7.

[12]Ganguli, B. N., and Bletzinger, P., "Shock Wave Dispersion in Nonequilibrium Plasma," AIAA Paper 96-4607, Nov. 1996.

[13]Vstovskii, G. V., and Kozlov, G. I., "Propagation of Weak Shock Waves in a Vibrationally Excited Gas," *Soviet Physics—Technical Physics*, Vol. 31, No. 8, 1986, pp. 911–914.

[14]Mnatsakanyan, A. K., Naidis, G. V., and Rumyantsev, S. V., "Shock Wave Propagation Through Nonuniform and Nonequilibrium Gas Regions," *Shock Waves and Tubes*, edited by H. Gronig, VCH, Weinheim, Germany, 1987, pp. 201–205.

[15]Bystrov, S. A., Ivanov, V. I., and Shugaev, F. V., "Propagation of Plane Shock Wave in Weakly Ionized Plasma," *Soviet Journal of Plasma Physics*, Vol. 15, No. 5, 1989, pp. 324–326.

[16]Herzfeld, K. F., and Litovitz, T. A., *Absorption and Dispersion of Ultrasonic Waves*, Academic, New York, 1959, Chap. 6.

[17]Raizer, Y. P., *Gas Discharge Physics*, Springer–Verlag, Berlin, 1991, Chap. 4.

[18]Liepmann, H. W., and Roshko, A., *Elements of Gasdynamics*, Wiley, New York, 1957, Chap. 3.

[19]Zel'dovich, Y. B., and Raizer, Y. P., *Physics of Shock Waves and High-Temperature Hydrodynamic Phenomena*, Academic, New York, 1967, Chap. 8.

[20]Demidova, N. S., Rukhadze, A. A., Fadeev, V. M., and Ebanoidze, Z. N., "Hydrodynamics of a Weakly Ionized Nonisothermal Plasma," *Soviet Physics—Technical Physics*, Vol. 30, No. 1, 1985, pp. 122, 123.

[21]Huxley, L. G. H., and Crompton, R. W., *The Diffusion and Drift of Electrons in Gases*, Wiley, New York, 1974, Chaps. 6, 8.

[22]Massey, H. S. W., Burhop, E. H. S., and Gilbody, H. B., "Electronic and Ionic Impact Phenomena," *Slow Collisions of Heady Particles*, Vol. 3, Clarendon, Oxford, England, UK, 1971, Chap. 18.

[23]Treanor, C. E., Adamovich, I. V., Williams, M. J., and Rich, J. W., "Kinetics of NO Formation Behind Strong Shock Waves," *Journal of Thermophysics and Heat Transfer*, Vol. 10, No. 2, 1996, pp. 193–200.

[24]Adamovich, I. V., Rich, J. W., and Nelson, G. L., "Feasibility Study of Magnetohydrodynamics Acceleration of Unseeded and Seeded Airflows," *AIAA Journal*, Vol. 36, No. 4, 1998, pp. 590–597.

[25]Avramenko, R. F., Rukhadze, A. A., and Teselkin, S. F., "Structure of a Shock Wave in a Weakly Ionized Nonisothermal Plasma," *Soviet Physics—JETP Letters*, Vol. 34, No. 9, 1981, pp. 463–466.

[26]Aleksandrov, N. L., Konchakov, A. M., and Son, E. E., "Electron Distribution Function and Kinetic Coefficients of a Nitrogen Plasma, I: Unexcited Molecules," *Soviet Journal of Plasma Physics*, Vol. 4, No. 1, 1978, pp. 98–102.

[27]Aleksandrov, N. L., Konchakov, A. M., and Son, E. E., "Electron Distribution Function and Kinetic Coefficients of a Nitrogen Plasma, II: Vibrationally Excited Molecules," *Soviet Journal of Plasma Physics*, Vol. 4, No. 5, 1978, pp. 663–666.

[28]MacDonald, D. K. C., *Thermoelectricity: An Introduction to the Principles*, Wiley, New York, 1962, Chap. 4.

[29]Gridin, A. Y., Klimov, A. I., Khodataev, K. V., Shcherbak, N. B., and Shcherbak, S. B., "Two-Dimensional Simulation of Shock Wave Propagation in a Transverse Pulse Glow Discharge with a Heated Cathode Layer," *High Temperature*, Vol. 32, No. 6, 1994, pp. 755–758.

[30]Kim, C. A., Jameson, A., Martinelli, L., and Xu, K., "An Accurate LED-BGK Solver in Unstructured Adaptive Meshes," AIAA Paper 97-0328, Jan. 1997.

[31]Adamovich, I. V., Subramaniam, V. V., Rich, J. W., and Macheret, S. O., "Shock Wave Propagation in Weakly Ionized Plasmas," AIAA Paper 97-2499, June 1997.

[32]Klimov, A. I., Gridin, A. Y., and Mishin, G. I., "Plasma Condensation Behind Shock Wave in Non-equilibrium Discharge and Ball Lightning," *Ball Lightning in Laboratory*, Khimiya, Moscow, 1994, pp. 175–183 (in Russian, English translation available upon request).

K. Kailasanath
Associate Editor